CFD SIMULATION OF LIQUID METAL FLOW IN A 19 ROD WRAPPED WIRE ASSEMBLY WITH FOCUS ON TURBULENT AND CONJUGATE HEAT TRANSFER

M. Böttcher, R. Krüssmann

Karlsruhe Institute of Technology, Institute for Neutron Physics and Reactor Technology, Hermann-von-Helmholtz-Platz 1, 76433 Eggenstein-Leopoldshafen, Germany
Post Box 3640, 76021 Karlsruhe, Germany

michael.boettcher@kit.edu

Abstract

In fast reactors, fuel assemblies with wire-wrapped rods are used, which allow a very compact arrangement of the fuel rods. The wrap induced swirl flow leads to increased mixing and enhanced heat transfer. To investigate the influence of turbulence modelling on the heat transfer, especially for fluids with low Prandtl numbers like sodium and LBE, a detailed CFD model was prepared. Special attention was given to optimize the mesh for accurate geometry representation and fast convergence. Simulations were run with three different turbulent Prandtl numbers (0.9, 1.5 and variable values generated by a look-up table method). It was found that the influence of the choice of Pr_t is low for fluids with very small Pr numbers like Na, while it is of much higher importance for fluids with a lower thermal conductivity. The conjugate heat transfer has a small impact at the touching zone between rod and wire.

1. INTRODUCTION

Within the Generation IV International Forum, the Sodium-cooled Fast Reactor was chosen as one possible concept to achieve sustainable development of nuclear energy. It is further developed in terms of performance of the core design, improved safety and resistance to accidents, and to optimize the power conversion system. The projected French reactor “Astrid” (acronym for “Advanced Sodium Technological Reactor for Industrial Demonstration”) shall demonstrate the technological progress in these fields at industrial scale, and at affordable costs (CEA, 2012).

Sodium has a higher thermal conductivity, but a lower heat capacity than water. Due to its high boiling temperature, the operational temperature window is very large (about 780 K) making it thermodynamically highly efficient as a coolant. Besides, there is no need for pressurization and it is not corrosive to steel. In comparison to water, neutrons are not slowed down in collisions, which is indispensable for the use in fast reactors.

Sodium cooled fast reactors have hexagonal-shaped fuel bundles. The rods are arranged in a triangular pattern and separated from each other by wrapped wires. The functionality of the wires is to preserve the geometrical arrangement of the rods and to improve the heat transfer conditions by enhanced mixing of the fluid between subchannels. Furthermore, the impact of conjugate heat transfer in rods and wires is of interest mainly in the contact zones. One of the most important design criteria in terms of safety is to keep the maximum temperatures of fuel and clad below a safety margin to the melting temperature.

In the framework of the European Project SESAME (Thermalhydraulics simulations and experiments for the safety assessment of metal cooled reactors), a local heat transfer model for wire-wrapped rod bundles is developed with the aim to predict the temperatures of fuel and clad accurately. For this purpose, also the mixing processes between the subchannels are investigated. A study with the commercial CFD program ANSYS CFX is undertaken with a detailed CFD model, so that the effects of turbulent mixing and conjugate heat transfer can be investigated separately. The objective is to extract local data for heat and mass transfer between subchannels.

This work is distributed into several parts: a) The computational model and in particular the mesh generation is presented. The mesh was optimized for fast convergence and geometrical accuracy. b) RANS simulations were performed for cases without heat transfer to test the model. The results for the

pressure loss are compared with correlations from literature. c) Simulations of heated cases including conjugate heat transfer were carried out for two constant turbulent Prandtl (Pr_t) numbers (0.9 and 1.5), and for Pr_t numbers derived by a so-called look-up table method based on LES/DNS channel flow data. d) The influence of conjugate heat transfer was investigated by comparing results for empty and full rods. In order to demonstrate the influence of the heat conductivity of the coolant, sodium is replaced by LBE, which means an increase of the molecular Prandtl number from 0.005 to approximately 0.016.

2. COMPUTATIONAL MODEL

A 19 rod bundle with wire-wrapped rods is chosen for this study. The geometry of the simulated bundle is related to the French Astrid design, which means a pitch-to-diameter (P/D) ratio of 1.11, a rod diameter of 9.6 mm and a wire diameter of 1mm, at a total length of 180mm representing one coil of the wires. The rod bundle is surrounded by a hexagonal channel. To accurately calculate the heat transfer, a dimensionless wall distance of the first cells of $y^+ \sim 1$ is required – this leads to spacings Δy at the wall of about 0.005 mm at Re=20000 for sodium flow and therefore to a high number of cells. On the other hand, the size of the model is limited by computer memory, and the computational time should be kept within one day for a steady state analysis. Mesh quality is though a crucial point. Especially the contact lines between rods and wires are challenging, but for a realistic calculation of the heat transfer they should be reproduced as good as possible. The contact zones between rods and wires are formed by tangencies, which makes the meshing of the real geometry difficult, so that modifications of the geometry are usually necessary. A study of possibilities such as radial replacement of the wire to the center of the rod, local degradation of the wire curvature to larger radii or transformation of the wires cross section from circular into rectangular shape is given by Bieder et al. (2010). Simplifications of the geometry are reducing the number of cells and the computational costs. Pointer et al. (2009) reduced the number of cells for a 217 fuel rods assembly from 44 million to 10 million cells by considering the wire shapes as rectangular. Rolfo et al. (2012) showed that the influence of geometrical modifications and the choice of cell types on the pressure loss is rather small ($\leq$4%), while the impact on the Nusselt number may be significantly larger (~15%). A very detailed representation of the discussed problems is given in the PhD thesis by Saxena (2014).

With the commercial meshing program Pointwise V18, a hybrid mesh was created, which is shown in Fig. 1. The geometry of the wires is mainly unchanged, while the contact line is considered as a contact surface at a width of 0.1mm. The resulting rectangular gap, see Fig. 2, is created by a fully structured block and considered as wire material (yellow). The coolant domain is indicated in blue, while rod material is colored in red. For the wire surfaces regular full structured hex elements are chosen, while the rod surfaces are meshed by hex dominant hybrid elements. Structured boundary layers were created by normal extrusion starting at mesh sizes of 0.005mm on the fluid side and of 0.01mm on the solid side by using growth rates of 1.3 (fluid) and 1.5 (solid). By this procedure a very good mesh quality could be achieved (minimum cell angle $\alpha > 20°$). The most challenging parts for meshing were formed by regions close to the contact zones inside the fluid domain, where the various structured layers are approaching each other. Here normal extrusion was stopped and it was left to the grid solver to build an unstructured mesh. In those regions the mesh quality is locally poorer ($\alpha_{min} \sim 4°$). Furthermore, especially for the fluid domain, the ratio in spacing between neighboring cells was kept mostly below a factor of 1.3 in order to increase numerical stability of the resulting numerical model. Finally, two versions of the model were created: The first one considers full rods leading to $107*10^6$ cells, while $70*10^6$ cells for the empty rod case were used. For sodium flow at Re=20000, y^+ values below 1.2 were obtained.

Due to practical reasons grid sensitivity studies were performed in a simplified way because the construction and testing of the presented model took several months and was not automated. For a Reynolds number of 20000, simulations were run by using a first order discretization method instead of a standard high order method. Only negligible changes in the results could be observed so that the grid was used for all cases.

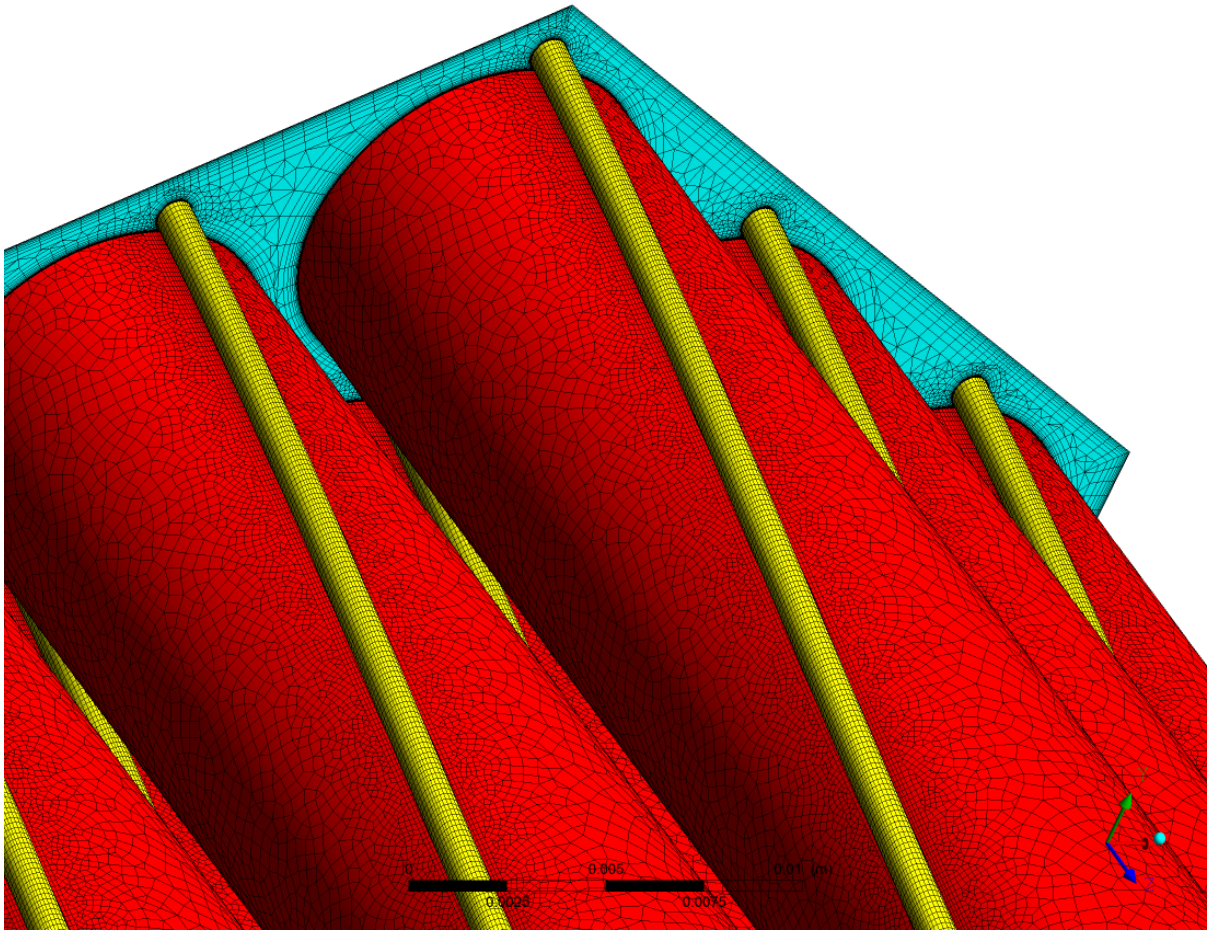

Fig. 1: The computational grid at the rod and wire surfaces

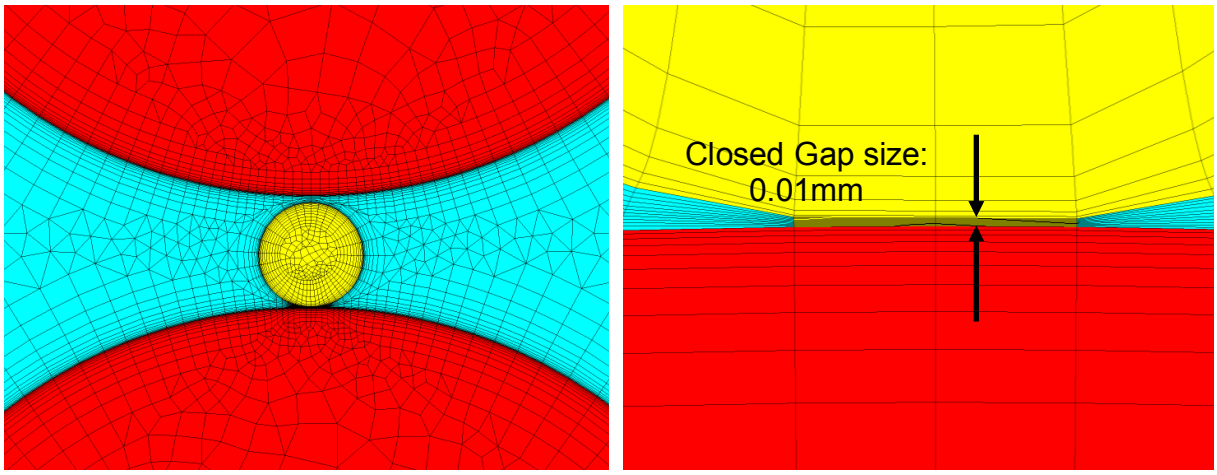

Fig 2: Mesh details around a wire (left) and in the touching zone (right)

For simplification, a single component, incompressible fluid (sodium) with temperature dependent properties and constant inlet temperature was simulated. The thermal properties are given in Sobolev (2011) and Fink and Leibowitz (1995). Gravitational forces were considered for all cases.

At the inlet 3D velocity components were set, obtained from a first run without heating, where an adequate mass flux condition at the inlet was applied. Then the 3D velocity distribution at the outlet was extracted and used as inlet condition for heated cases. It has to be mentioned that for unheated cases axial periodicity between inlet and outlet can be applied, but heated cases may be only quasi periodic because of the temperature dependent properties. For the turbulence intensity at the inlet a value of 1% is applied. At the outlet, an averaged relative pressure of 0 Pa was set. The assembly walls and the upper and lower front planes of the rods and wires are treated as adiabatic.

In case of empty rods, a constant heat flux of 10^6 W/m^2 (at Re_0=38900) at the fluid-rod boundary is applied. For other Re the heat flux is linearly scaled by Re, so that the average temperature increase between inlet and outlet is constant. For solid rods a constant volumetric heat source is applied with the same scaling procedure.

Turbulence was considered by an ω-Reynolds Stress (RS) model by Wilcox (1986), because anisotropic effects can be better handled. Apart from the rod and wire touching lines each subchannel gets locally nearly completely blocked by approaching wires from neighboring rods that causes local anisotropy.

For the simulation of turbulent energy transport, a Reynolds analogy is applied. This means that eddy viscosity and turbulent thermal diffusivity are connected by the so called turbulent Prandtl number Pr_t given by

$$Pr_t = \frac{\nu_t}{a_t} = \rho c_p \frac{\nu_t}{\lambda_t} \quad (1).$$

Eddy viscosity is calculated by solving partial differential equations for all components of the Reynolds stress tensor (full RS models) or by simplified two equation turbulence models, and then the turbulent thermal conductivity is obtained by eq. (1), which assumes isotropy for the turbulent heat transfer. For Pr_t, usually a standard value of 0.9 is used which implies similarity between viscous and thermal boundary layers. In reality, Pr_t is a highly complex function and depends on the flow type, on the wall distance y^+, dimensionless numbers like the Prandtl number Pr, the Reynolds number Re, and the Grashof number Gr, and for transient flows on time, also. For liquid metal flows with very small Prandtl numbers (down to 0.005 for sodium), the thermal boundary layers are significantly larger than the momentum layers and the uncertainty in the available data and correlations is large. In literature, a number of semi-empirical correlations is available (Kays, 1992).

Simulations of heated cases for Re from 5000 to approximately 40000 were carried out considering conjugate heat transfer and three different turbulent Prandtl numbers Pr_t of 0.9, 1.5, and a so called look-up-table method. This method by Böttcher (2014) is based on LES/DNS 2D channel flow data. The extracted Pr_t profiles from those simulations are arranged in a 3D table with a dependency on y^+, Re and the molecular Prandtl number. Then for each point of the fluid domain a value for Pr_t is calculated from the values within this table by 3D linear interpolation. For this procedure Re at the assembly inlet is used, furthermore molecular Prandtl numbers based on local fluid properties. The main problem is the specification of a 3D distribution for y^+, because the used CFD solver ANSYS CFX 17 provides only a distribution of y^+ at the domain walls. Furthermore, at the very first iteration y^+ is unknown. So y^+ was taken from previous simulations with constant Pr_t, because usually variations of Pr_t have only a negligible influence on y^+. The look-up table method works well at forced convection and channel type flows. Validation was performed for pipe flow and rod bundle flow including spacers in Böttcher (2014). Limitations are mainly given by upcoming buoyancy effects because no gravity influence is presently implemented in the data tables. The look-up table data base presently contains data by Kawamura et al. (1999), Duponcheel et al. (2013) and by Kawamura Lab (2017). The data covers an approximate range for Re between 5000 and 80000 and for Pr between 0.01 and 10. In case of sodium flow Pr is close to 0.005, so that Pr=0.01 was used to calculate the look-up table method values.

Steady state RANS simulations for heated cases were carried out for the previously mentioned Reynolds number range with an empty rod model version. In order to study the influence of conjugate heat transfer mainly on the hot spot in the contact zones a full rod model was created additionally. Finally, sodium was replaced by LBE with the intention to demonstrate the influence of molecular thermal conductivity, which is more than a factor of 3 smaller for LBE.

High level convergence criteria of 10^{-5} for RMS residuals and 0.1% for global balance targets were applied, which were reached after 90 iterations. Even a criterion of 10^{-6} could be reached, but since monitoring values remained constant, the computational effort was unnecessary. A heated case for the empty rod model consumed about 8 CPU h (24 CPU ś, 2.5 GHz, Intel Xeon).

3. RESULTS

The model was tested first without heating. The pressure loss was investigated by calculating the friction factor defined as

$$\xi = \frac{-\frac{\Delta p}{L}}{\frac{1}{2}\rho u^2} D_h \qquad (2).$$

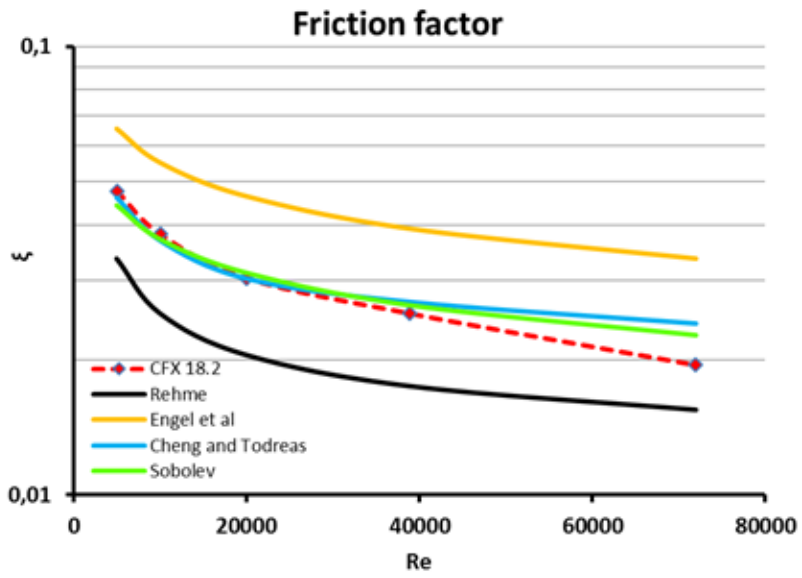

Fig. 3: Friction factor over Reynolds number for the unheated bundle

L is the length of the bundle, D_h is the hydraulic diameter and u a cross section averaged axial velocity.

As can be seen in Fig. 3, the correlations of Cheng and Todreas (1986) and Sobolev (2006) fit well with the simulation results, while Rehme (1973) and Engel et al. (1979) rather present lower and upper boundaries, respectively. For Re>40000 the CFX simulations approach the Rehme correlation.

The heat transfer is signifycantly more difficult to predict, and the variations in correlations found in literature are large, even in the latest publications. In Fig. 4 the Nusselt number for some selected rods defined as

$$Nu = \frac{\alpha D_h}{\lambda} = \frac{q'}{(T_{Rod} - T_{Bulk})} \frac{D_h}{\lambda} \qquad (3)$$

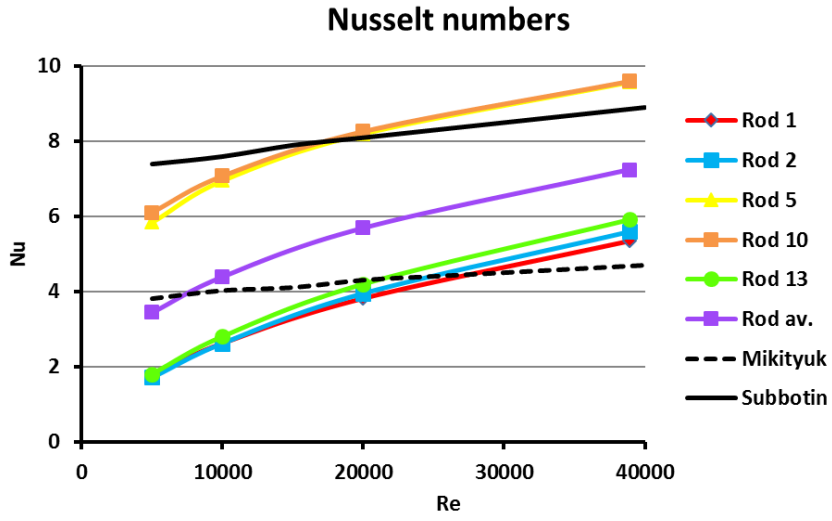

Fig. 4: Nusselt number over Reynolds number

is shown. The rod positioning is presented in Fig. 5. As bulk temperature, the cross sectional averaged temperature of the subchannel surrounding each individual rod is used. For the hydraulic diameter D_h, values for the local subchannel cross sections are used. The bulk temperature T_{Bulk} and the thermal conductivity λ are mass flow averaged values also taken from local subchannel cross sections. The wall temperature at each rod surface is calculated by linear circumferential averaging at a constant axial position. This procedure was performed at four different axial levels at normalized positions between 0.1 and 0.9 in order to avoid the impact of the boundary conditions. The final values are calculated by an averaging over the just mentioned four axial levels.

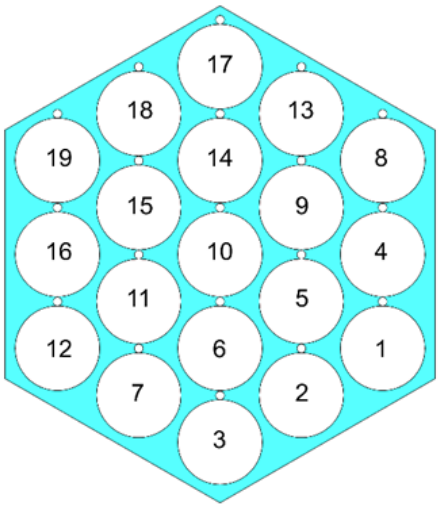

Fig. 5: Rod positioning

For the simulations, a standard value of Pr_t=0.9 is assumed. The results are within the range limited by the correlations from Mikityuk (2009) and Subbotin (1975). It has to be mentioned that the correlations are representing an average for an entire bundle while here results for individual rods are shown. Building an averaged value for the entire assembly shifts the results for all Re clearly into the range formed by the correlations. For the central rod 10 the highest Nusselt numbers are predicted. It is surrounded everywhere by neighboring rods covered by wire wraps which are responsible for swirl flow with velocities up to 40% of the main axial flow. This leads to the best mixing conditions in the bundle. Its next neighbor, rod 5 shows about 5% lower values because an influence of the outer assembly wall becomes visible. For rod 1 and 2, which are on the edge near the wall or in the corner of the wrapper, respectively, the heat transfer is significantly reduced. The better heat transfer conditions for rod 1 compared to rod 2 may be explained by a stronger swirl flow in the corner region together with the lowest number of local subchannel blockages by neighboring wires.

The results can be better understood by a detailed analysis of the velocity field, see Fig. 6. Velocity values are normalized by the cross section averaged axial velocity. The pictures are taken at different axial positions z*, which is the axial coordinate normalized by the total model assembly length. Due to the wire wrap induced swirl flow the mass flow distribution is highly 3D and the maximum of the main flow component w in axial direction is shifted to subchannels close to the assembly wall. The circumferential maxima depend on the wire position and therefore on the axial position. The swirl flow may reach local maxima close to 40% of the axial flow and it has significant impact on transport processes. The largest swirl components are calculated close to local blockings of the wire wraps.

In Fig. 7, the surface rod temperature and the temperature distribution at the inlet and outlet are presented. At the inlet for all cases a constant coolant temperature of 623 K is assumed, while at the outlet an average temperature of about 653 K is reached. The hottest rod is located at the central position, at all sides surrounded by other rods and has the lowest axial mass flow in its touching subchannel. A constant heat flux means that the highest Nusselt number for this rod corresponds with the lowest temperature difference between rod and bulk temperature. Local temperature maxima exist at the touching lines between rod and wire and where wires come close to the surface of neighboring rods and locally block the subchannels. This is visible at the outlet cross section.

The temperature distribution for the same case in Fig. 8 is taken at the axial center of the assembly between rod 10 and rod 6. Inside the wire, where the contact zone with sodium and rod is indicated as black line, conjugate heat transfer is considered. The wires material is assumed as steel with a thermal conductivity of 15.5 W/m K. At the contact zone between wire and rod a local temperature increase of about 15 K is calculated. The partial blocking of the subchannels only leads to a local surface temperature increase <4K at rod 6 (lower position).

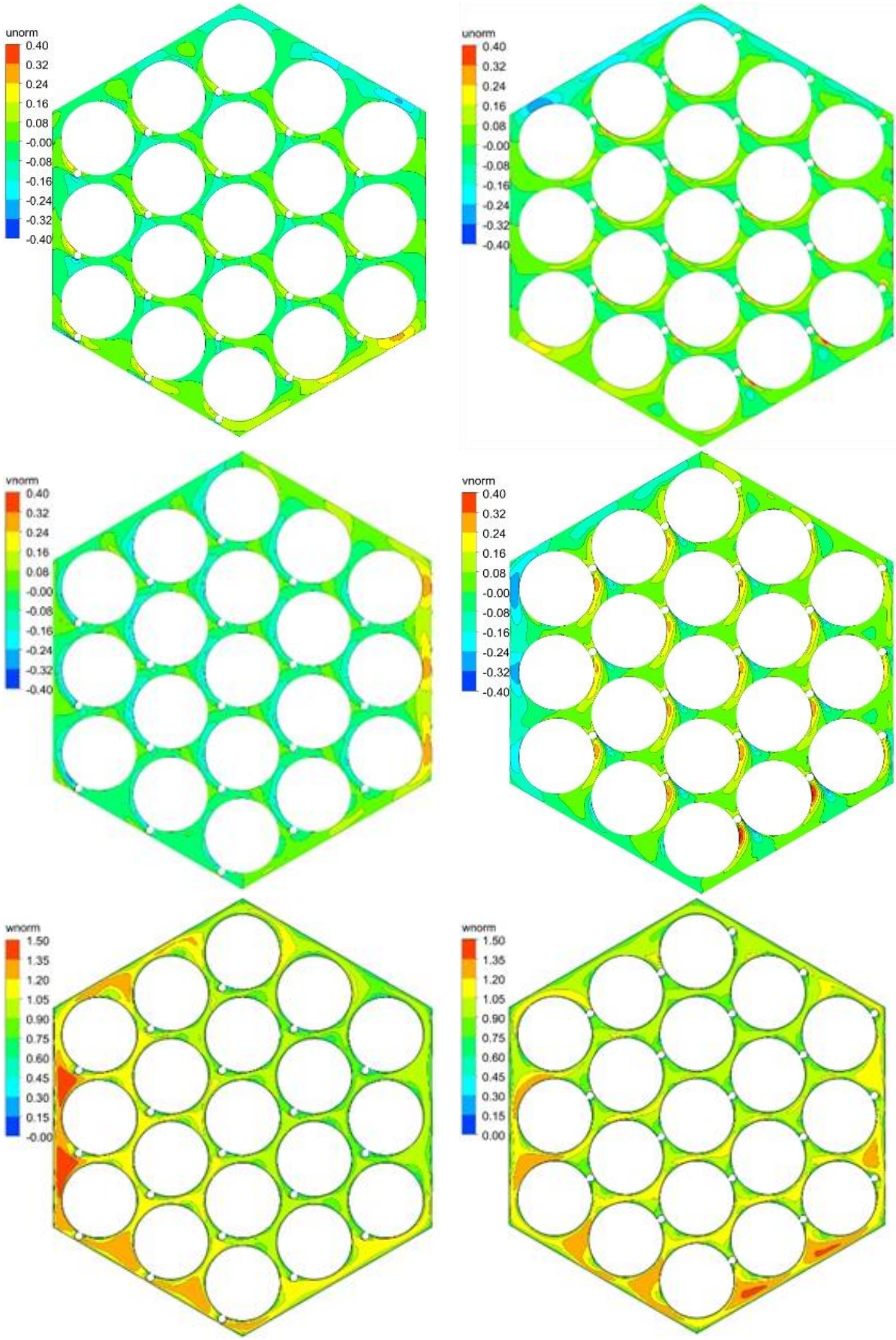

Fig. 6: Normalized velocity components at z*=0.417 (left column) and z*=0.833 (right column) at Re=38900

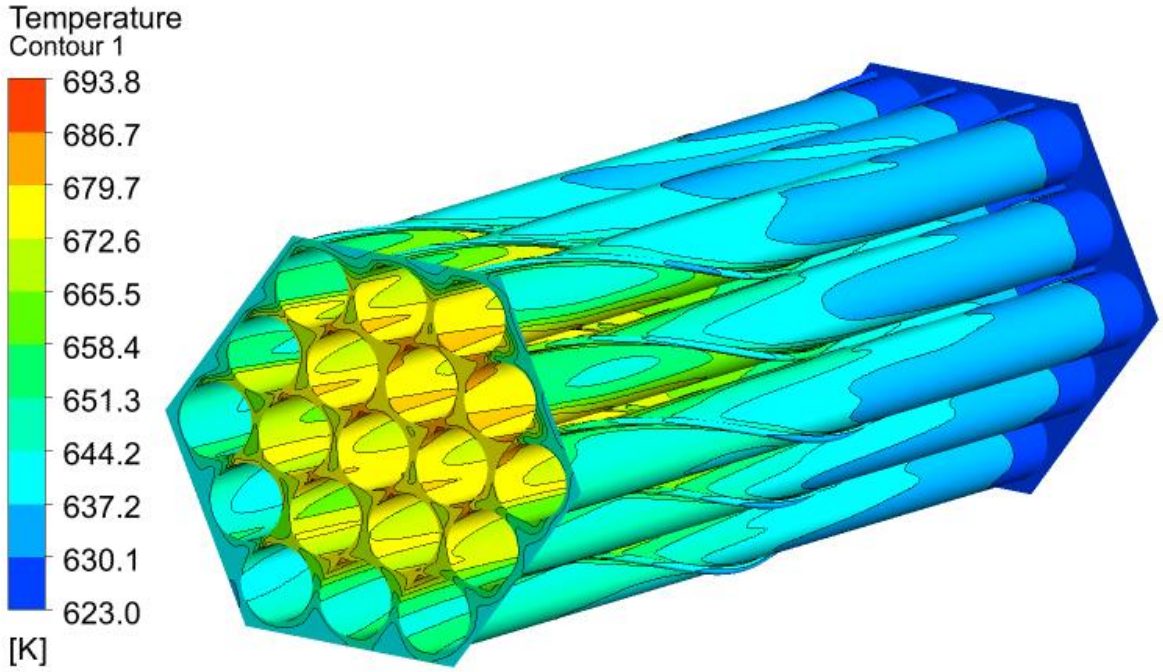

Fig. 7: Rod surface temperature (Q=10^6 W/m^2 , Re=38900)

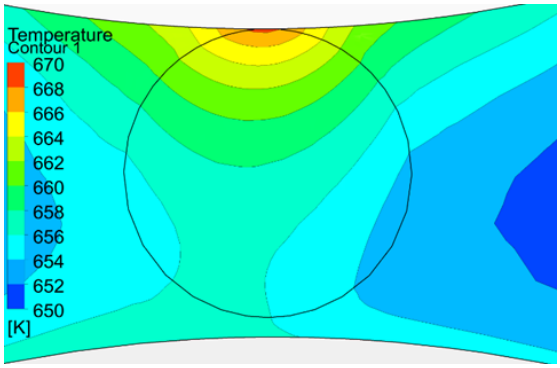

Fig. 8: Temperature distribution at central rod (z*=0.5, Re=38900, 10^6 W/m^2)

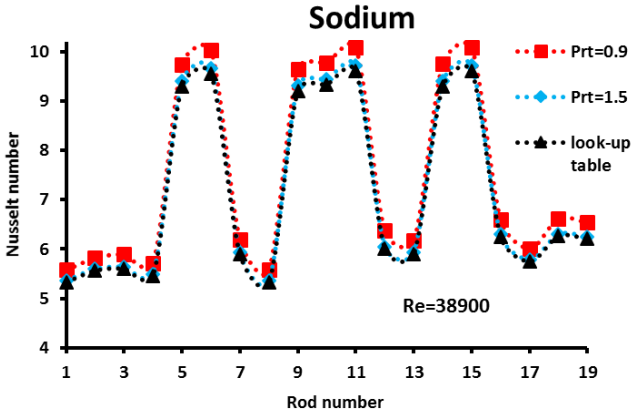

Fig. 9: Nusselt numbers at different Pr_t

Fig. 9 shows rod specific Nusselt numbers at Re = 38900 and for different Pr_t ś of 0.9, 1.5 and by the look-up table method, for which the Pr_t distribution is given by Fig. 10. The distribution is taken in central axial position of the assembly and focused on the central rod. In liquid metal flows values for Pr_t may be significantly >1, especially close to walls, where values >5 can be reached. In a small layer close to the walls values up to 4 are obtained, while in the direction of the center of the subchannels the values are decreasing and moving towards 1.

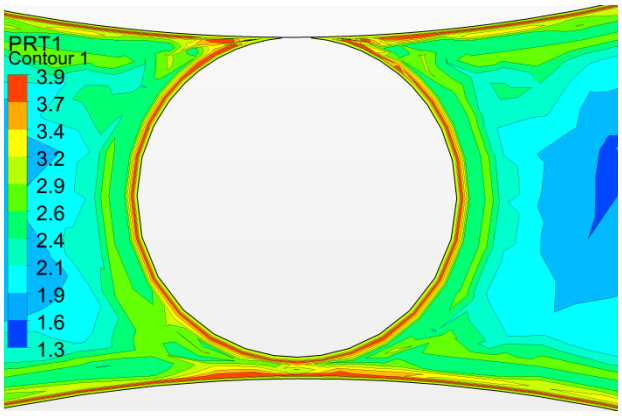

The influence of Pr_t, which means the influence of the turbulent heat transfer, is moderate because of the very high molecular heat conductivity of sodium. Using a more realistic value for Pr_t of 1.5 instead of 0.9 leads to a decrease of Nu of about 4%. Using the probably best values for Pr_t by the look-up table method does not lead to additional modifications/improvements because of the low influence of turbulent heat transfer.

Fig. 10: Pr_t distribution by look-up table method

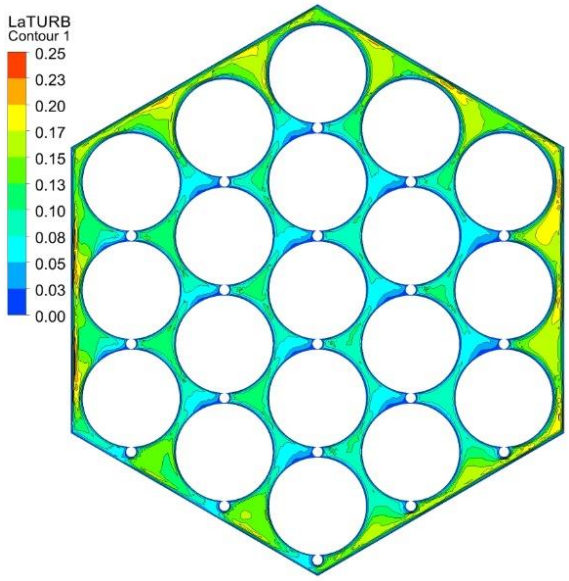

Fig. 11: λ_t/λ for sodium flow at Re=38900

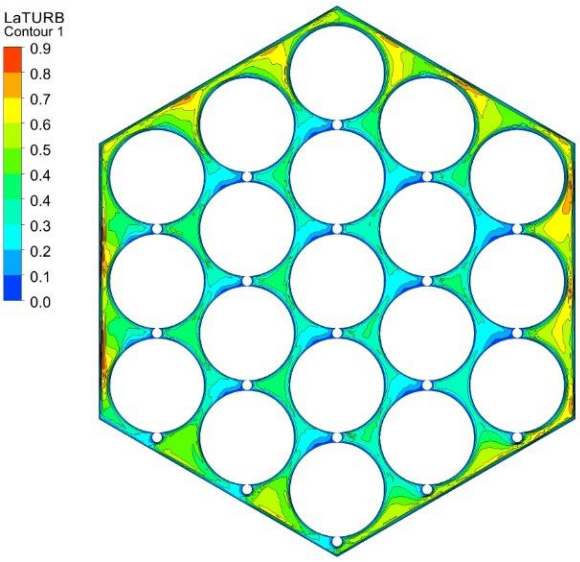

Fig. 12: λ_t/λ for LBE flow at Re=38900

The importance of the turbulent heat transfer against molecular conduction can be demonstrated by an analysis of the ratio of turbulent conductivity to molecular conductivity shown in Fig. 11 and 12 for sodium and LBE, respectively. The data is taken in central axial position of the assembly. It has to be mentioned that LBE is treated also with temperature dependent properties following the HLMC handbook (2007) by OECD. Table 1 gives a comparison of some properties of sodium and LBE. While sodium has a conductivity >50 W/m K, the value for LBE is below 15 W/m K, so that turbulent heat transfer in case of LBE is much more important. In case of sodium the ratio λ_t/λ is mostly <0.1, this means molecular conduction is dominant. For LBE the ratio is significantly larger due to the lower conductivity. For both cases the highest ratios are predicted in regions close to the adiabatic assembly wall, where temperature gradients are small. Therefore, a more accurate prediction of the turbulent heat transfer is much more important for metals with lower conductivity than for sodium flow.

An analysis of rod individual Nusselt numbers at different turbulent Prandtl numbers for LBE flow is presented in Fig. 13. The results can be directly compared with those for sodium given in Fig. 8, but one has to take into account that the Péclet number for the LBE case is higher (700 instead of 200 for the sodium case). The heat flux was chosen so that the average heat up between inlet and outlet is the same for both fluids. By keeping the geometry for both cases it is not possible to preserve Re and the Péclet number simultaneously because of the different physical properties of the materials presented in Table 1. As consequence of a higher Pe the values for Nu have increased by about 40%. The focus of this part of the study is mainly on the relative influence of different turbulent Prandtl numbers. At the peripheral

rod positions, variations of Nu up to 10% are calculated now. For the central rod the relative differences increase up to 15%. This is more than three times higher compared with the sodium case. The importance of modelling turbulent heat transfer increases when a fluid with lower thermal conductivity is used.

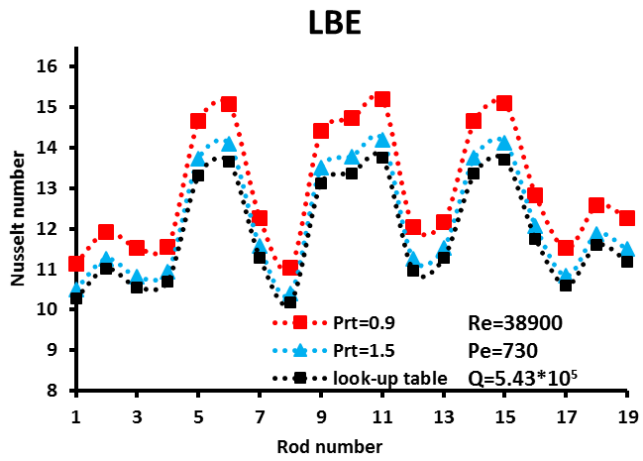

Fig. 13: Rod individual Nu numbers for LBE flow

	Sodium	LBE
ρ [kg/m^3]	866.66	10274
Cp [J /kg K]	1279.69	145.87
λ [W/ m K]	75.28	12.73
η [Pa s]	3.04*10^{-4}	0.0017
Pr	0.0052	0.0197

Table 1: Properties for Sodium and LBE at T_0 = 623 K

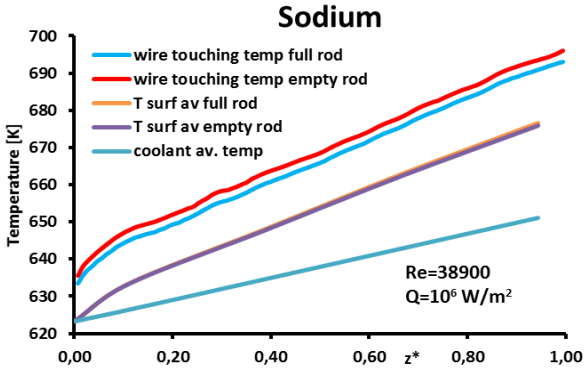

Fig. 14: Sodium flow

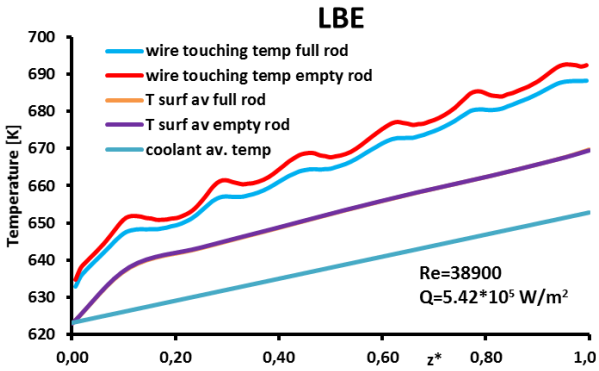

Fig. 15: LBE flow

Fig. 14 and Fig. 15 are showing averaged coolant temperatures at different axial positions and the central rod circumferential averaged surface temperatures. Furthermore, for the central rod the temperatures in the touching line between rod and wire are presented. At the same Reynolds number, the heat flux is selected in a way that the average axial heat up is the same for sodium and LBE. All cases are calculated by using the look-up table method.

For both fluids the average rod temperatures are nearly identical for the empty and full rod model. In case of sodium, the temperature of the hot spot at the touching line is about 3K higher for the empty rod case compared with the full rod case. The temperatures here are predicted to be up to 15K hotter than on the other part of the rod surface at the same axial position. In case of LBE, the local temperature increase in the touching line is calculated to be up to 20K for the full rod model and 25K for the empty rod model, respectively. This can be explained again by the significantly lower conductive transport in LBE.

Oscillations of the touching line temperature data can be explained by local subchannel blockages of neighboring wires. Smaller oscillations are also visible in the sodium case but they are damped by energy transport due to larger molecular conduction.

The influence of conjugate heat transfer is mainly visible on the calculation of local hot spots, while the impact on averaged quantities like Nusselt numbers is small. Lower thermal conductivity increases local temperature maxima.

4. CONCLUSIONS AND OUTLOOK

A CFD model with an optimized grid for a 19 rod assembly with P/D=1.11 was developed. Care was taken to obtain a high quality grid together with a nearly accurate representation of the geometry. Good numerical performance and convergence behavior was obtained. Sodium and LBE flow were calculated to investigate the influence of the turbulent Prandtl number on turbulent heat transfer and conjugate heat transfer along the touching zones of the wires. Results for pressure loss and overall heat transfer are in good agreement with correlations found in literature. Calculations of Nusselt numbers for individual rods show a significant influence of the rod position on the heat transfer conditions.

The studies have shown a local impact of conjugate heat transfer mainly on the local maxima of the temperatures at the touching zones between rods and wires. The choice of a suitable turbulent Prandtl number has low influence on the heat transfer results in case of a fluid with high thermal conductivity as e.g. sodium. For other materials like LBE with lower conductivity turbulent heat transfer modelling is of higher importance.

Within the SESAME project local data generated by the presented CFD model will be used for the development of correlations for momentum and energy exchange between subchannels to be implemented within system tools. In order to extend the data basis, it is planned to create similar models with other P/D ratios.

Acknowledgement

The presented work was supported by the European Union within SESAME project under the Grant Agreement Number 654935.

REFERENCES

U. Bieder et al., “CFD Calculations of wire wrapped fuel bundles: modelling and validation strate-gies“, CEA-Grenoble, DEN/DER/SSTH/LDAL, (2010).

M. Böttcher, “CFD Simulation of heat transfer in liquid metal flow by using an innovative Re analogy approach”, Proc. CFD4NRS-5, Zürich, Switzerland, Sept. 9-11, (2014).

CEA, Nuclear Energy Division (Ed.), “4th – Generation sodium-cooled fast reactors: The ASTRID technological demonstrator”, (2012).

S. Chen and N. Todreas, “Hydrodynamic models and correlations for bare and wire-wrapped hexagonal rod bundles – bundle friction factors, subchannel friction factors and mixing parameters”, Nuclear Engineering and Design, 92 (2), 227–251 (1986).

M. Duponcheel, L. Bricteux, M. Manconi, G. Winckelmans, Y. Bartosiewicz, “Numerical Simulation of Liquid Metal Heat Transfer at High Reynolds Number”, Proc. Nureth-15, Pisa, Italy, May 12th-17th, 299 (2013).

F.C. Engel et al., “Laminar, transition and turbulent parallel flow pressure drop across wire-wrap spaced rod bundles”, Nuclear Science and Engineering, 69 (2), 290-296 (1979).

J.K. Fink, L. Leibowitz, “Thermodynamic and transport properties of sodium liquid and vapor”, Technical report ANL/RE-95/2, Argonne National Lab, IL (United States) (1995).

GenIV International Forum, https://www.gen-4.org/gif/jcms/c_9260/public

Handbook on Lead-bismuth Eutectic Alloy and Lead Properties, Materials Compatibility, Thermal-hydraulics and Technologies (OECD-NEA 6195), Paris, Frankreich, 2007. URL: www-pub.iaea.org/MTCD/Publications/PDF/ P1567_web.pdf [Stand: 19.09.2013].

H. Kawamura, H. Abe, Y. Matsuo, “DNS of turbulent heat transfer in channel flow with respect to Reynolds and Prandtl number effects”, Int. J. of Heat Fluid Flow, 20 (3), 196-207 (1999).

Kawamura Lab, Tokyo University of Science, DNS Database of Wall Turbulence and Heat Transfer, www.rs.tus.ac.jp/~t2lab/db/index.html, (2017).

W.M. Kays, “Turbulent Prandtl Number- Where Are We?”, Max Jacob Memorial Award Lecture 1992, J. Heat Transfer, 116(2), 284-295 (1994).

K. Mikityuk, “Heat transfer to liquid metal: Review of data and correlations for tube bundles”, Nuclear Engineering and Design, 239(4), 680-687 (2009).

W.D. Pointer, J. Thomas, T. Fanning, P. Fischer, A. Siegel, J. Smith, A. Tokuhiro, “RANS based CFD simulations of sodium fast reactor wire-wrapped pin bundles”, International conference on Mathematics, Computational Methods and Reactor Physics, American Nuclear Society, Saratoga Springs, May 3rd – 7th, 2212 – 2224 (2009).

K. Rehme, “Pressure drop correlations for fuel element spacers”, Nuclear Technology, 17(1), 15-23 (1973).

S. Rolfo et al., “Thermal-hydraulic study of a wire spacer fuel assembly”, Nuclear Engineering and Design, 243, 251-262 (2012).

A. Saxena, “Thermal-hydraulic numerical simulation of fuel sub-assembly for Sodium-cooled Fast Reactor”, University of Marseille, PhD thesis (2014).

Sobolev V., “Fuel Rod and Assembly Proposal for XT-ADS Pre-design“, Coordination meeting of WP1&WP2 of DM1 IP EUROTRANS, Bologna, 8-9 February, (2006).

V. Sobolev, “Database of thermophysical properties of liquid metal coolants for GEN-IV”, SCK-CEN, Mol, Belgium, BLG-1069 (2011).

V. I. Subbotin, P. A. Ushakov, A. V. Zhukov, N.M. Matyukhin, Yu. S. Yur’ev and L.K.Kudryavtseva, “Heat transfer in cores and blankets of fast breeder reactors”, Proceedings of Second Symposium of Member Nations of Council for Mutual Economic Aid, State and Prospects of Work on the Construction of Atomic Power Stations with Fast Neutron Reactors, October 1973, Obninsk, Russia, Vol. 2 (1975).

D.C. Wilcox, “Multiscale model for turbulent flows”, Proc. AIAA 24th Aerospace Sciences Meeting, January 6th – 9th, Reno (Nevada, USA), American Institute of Aeronautics and Astronautics (1986).